TECHNICAL MEMORANDUMS

NATIONAL ADVISORY COMMITTEE FOR AERONAUTICS

No. 578

CALCULATION OF TAPERED MONOPLANE WINGS

By E. Amstutz

From Schweizerische Bauzeitung, April 5, 1930

Washington
August, 1930

NATIONAL ADVISORY COMMITTEE FOR AERONAUTICS.

TECHNICAL MEMORANDUM NO. 578.

CALCULATION OF TAPERED MONOPLANE WINGS.*

By E. Amstutz.

For some time there have been built in increasing numbers monoplanes with cantilever wings, which no longer have the customary rectangular or elliptical contour, but are decidedly tapered. The flying boat "Romar," built by the Rohrbach Company, is a striking example of this type (Fig. 1).

Obviously this shape increases the lift in the middle of the wing and thus reduces the bending moment of the lifting forces in the plane of symmetry. Since this portion of the wing is the thickest, the stresses of the wing material are reduced and desirable space is provided for stowing the loads in the wing. This statically excellent form of construction, however, has aerodynamic disadvantages which must be carefully weighed, if failures are to be avoided. This treatise is devoted to the consideration of these problems.

The wing theory, as developed principally by Prandtl,** shows that the resistance forces of a wing can be divided into two sharply distinguished portions. First there is the so-called profile drag, which is produced by the skin friction and separa-

*"Zur Berechnung von spitzendigen Eindecker-Tragflügeln," Schweizerische Bauzeitung, April 5, 1930, pp. 181-186.

**L. Prandtl, "Tragflügeltheorie I and II," in Vier Abhandlungen zur Hydrodynamik und Aerodynamik, Göttingen, 1927.

tion of the boundary layer. It depends on the profile form and on the total area, but not on the particular plan form, with which we accordingly have nothing further to do. The second portion, which alone interests us here, is produced by the secondary motions imparted to the air by the wing, which thus supports the weight of the whole airplane. Since there is energy in the secondary motion, the wing must experience a resistance, which is termed (not very aptly) the "induced" drag.

The induced drag is produced somewhat as follows. The air over which the wing moves receives a downward thrust, the nearer layers of air receiving a more vigorous impulse and the more remote layers a less vigorous impulse. Through the yielding of the downward impelled air masses, lateral and upward currents are produced near the wing tips, thus causing, in connection with the downward motion below and above the wing, a circulation about the wing tips which, due to the inertia of the air, extends as an elongated vortex system over the whole flight path. The wing itself lies in a downward flow which it has produced and up which it must climb as up an inclined plane. An element of the wing (Fig. 2) is not met by this upward flow in a direction opposite to the flight speed V, but at an angle smaller by w/V (measured in absolute mass), w denoting the downward velocity of the induced motion at the location of the wing element. The hydrodynamic lift is then perpendicular not to V, but to the resultant speed, so that, with respect to the flight direction, the component Aw/V offers a resistance, namely, the

induced drag W_i.

The magnitude of the downward velocity w at every point of the wing depends on the lift distribution along the wing span. Prandtl and Munk have shown that the energy of the secondary flow, and hence the induced drag, is the smallest when the lift is distributed over the span in the form of a half-ellipse. The downward velocity w is then along this constant, whereby the mathematical treatment of the resistance problem is much simplified, since it then reverts to the solution of an easily solvable potential problem. Moreover, this minimum theorem is very generally applicable and can be used for complicated wing systems.

Every nonelliptical lift distribution generates downward velocities, which are the greatest in the middle or at the tips of the wing, according to whether they are fuller or less full than the elliptical. Since the downward velocity affects the flow direction of the individual wing elements, it also affects the lift distribution and, due to this interchange, offers considerable difficulty to the determination of the induced drag for any given wing shape. The rectangular wing was very accurately treated by Betz,* the result of whose investigation is represented in Figure 3.

*"Beiträge zur Tragflügel-Theorie mit besonderer Berücksichtigung des einfachen rechteckigen Flügels," Göttingen dissertation, published in Munich in 1919.

The lift distribution on tapered wings can be represented with sufficient accuracy for practical purposes by a series with only three terms. In the present treatise, it is first shown how, for such a lift distribution, the wing shape producing it can be found. For this purpose, the distribution of the bending and torsional moments of the air forces along the span are determined, and the formulas for the comparison of the drag and maximum bending and torsional moments of tapered and elliptical wings are given. An example of a warped wing shows how the lift distribution for a given wing can be found approximately by solving two linear equations. The simplified equations are given for an unwarped wing.

Notation

x	distance from axis of symmetry (m).
b	span (m).
$\xi = \frac{2x}{b}$	
t	chord at distance x (m).
V	flight speed (m/s).
w	vertical induced velocity (m/s).
γ	angle of attack.
δ	angle of decalage.
ρ	air density (kg $m^{-4}s^2$).
$q = \frac{\rho^2}{2}$	= dynamic pressure (kg/m^2).

F projected wing area (m^2).

A total lift of wing (kg).

W total drag of wing (kg).

W_p profile drag (kg).

W_i induced drag (kg).

M moment of air forces about intersection point of vertical line from foremost point of wing profile with chord (m kg).

c_a defined by $A = c_a\ qF$

c_w " " $W = c_w\ qF$

c_{wp} " " $W_p = c_{wp}\ qF$.

c_{wi} " " $W_i = c_{wi}\ qF$

c_m " " $M = c_m\ qFt$

B bending moment (m kg).

T torsional " (m kg).

Γ circulation in m^2/s defined as

$$\Gamma = \frac{\text{lift per m span}}{\rho\ V} = c_a\ Vt$$

α, β coefficients.

All values which apply to the center of the wing ($x = \xi = o$) have the index o.

Prandtl gives .....

$$\Gamma = \Gamma_o \sqrt{1 - \xi^2}\ (1 + \alpha\ \xi^2 + \beta\ \xi^4 + \ldots) \qquad (1)$$

as the proper function to represent the lift distribution. We will confine ourselves to the use of the first three terms.

Examples of lift distribution, thus obtained, are plotted in Figures 4a, 4b, and 4c. For the elliptical distribution $\alpha = \beta = 0$, while less full distributions, applicable to tapered wings, yield negative values of α. From the above-mentioned source we also take

$$A = \frac{\pi}{4} \rho\, b\, V\, \Gamma_o \left(1 + \frac{\alpha}{4} + \frac{\beta}{8}\right) \tag{2}$$

$$w = \frac{\Gamma_o}{2b} \left[1 + \alpha \left(3\,\xi^2 - \frac{1}{2}\right) + \beta \left(5\,\xi^4 - \frac{3}{2}\,\xi^2 - \frac{1}{16}\right)\right] \tag{3}$$

$$W_i = \frac{\pi\rho}{8} \Gamma_o^2 \left(1 + \frac{\alpha}{2} + \frac{\beta}{4} + \frac{\alpha^2}{4} + \frac{11}{32}\,\alpha\,\beta + \frac{1}{128}\,\beta^2\right) \tag{4}$$

and taking equation (2) into consideration

$$W_i = \frac{A^2}{\pi q\, b^2} \frac{\left(1 + \frac{\alpha}{2} + \frac{\beta}{4} + \frac{\alpha}{4} + \frac{11}{32}\,\alpha\,\beta + \frac{\beta^2}{128}\right)}{\left(1 + \frac{\alpha}{4} + \frac{\beta}{8}\right)^2} \tag{4a}$$

The bending and torsional moments are also of interest. For the bending moment in x_1 or ξ_1 (Fig. 5) we obtain

$$M_{x_1} = \int_{x_1}^{x=b/2} (x - x_1)\, d\, A \tag{5}$$

$$= \rho\, V\, \frac{b^2}{4}\, \Gamma_o \int_{\xi_1}^{\xi=1} \sqrt{1 - \xi^2}\, (1 + \alpha\,\xi^2 + \beta\,\xi^4)\, (\xi - \xi_1)\, d\,\xi$$

On substituting $\xi = \sin\varphi$, we obtain, after several transformations

$$M_\xi = \rho V \frac{b^2}{4} \Gamma_o \left[\sqrt{1 - \xi^2} \left\{ \left(\frac{1}{3} + \frac{\xi^2}{6} \right) + \alpha \left(\frac{2}{15} - \frac{7}{120} \xi^2 + \frac{1}{20} \xi^4 \right) + \beta \left(\frac{8}{105} - \frac{41}{1680} \xi^2 - \frac{11}{840} \xi^4 + \frac{1}{42} \xi^6 \right) \right\} - \xi \left(\frac{1}{2} + \frac{\alpha}{8} + \frac{3}{48} \beta \right) \arccos \xi \right] \qquad (6)$$

and, especially for the moment in the center of the wing,

$$M_o = \rho V \frac{b^2}{12} \Gamma_o \left(1 + \frac{2}{5} \alpha + \frac{8}{35} \beta \right) \qquad (7)$$

and, taking account of equation (2)

$$M_o = \frac{Ab}{3\pi} \frac{1 + \frac{2}{5} \alpha + \frac{8}{35} \beta}{1 + \frac{1}{4} \alpha + \frac{1}{8} \beta} \qquad (7a)$$

The torsional moment cannot be represented by this general equation. As shown below, the circulation distribution does not definitely determine the shape of the wing. Hence the torsional moment is also affected by other limiting assumptions.

Determination of the Shape of a Wing for Producing a Given Lift Distribution

We now proceed to the solution of the problem as to what wing shape will give the desired lift and circulation distribution $\Gamma(\xi)$.

A wing is characterized by its plan form or contour $t(\xi)$, its profile and its warping $\delta(\xi)$. An element of the wing should

show the circulation

$$\Gamma = \Gamma_0 \sqrt{1 - \xi^2}\,(1 + \alpha\,\xi^2 + \beta\,\xi^4) = \frac{c_a}{2}\,V\,t \qquad (8)$$

The necessary chord t is thus fixed when c_a is given. For a given profile, c_a is affected only by the angle of attack, as is obvious from profile books on the basis of experimental results. In the practical range $c_a\,(\gamma)$ may be assumed to be linear by putting $\Delta\,c_a = k\,\Delta\,\gamma$. Theoretically, $k = 2\pi$ for thin slightly cambered wings, but somewhat smaller values are obtained experimentally.

If the middle of the wing has a geometrical angle of attack $\gamma_{\infty\,0}$, that is, if the wing is warped at ξ by an angle δ, that is, δ^0 steeper than in the middle of the wing, its geometrical angle is

$$\gamma_\infty = \gamma_{\infty\,0} + \delta$$

The index ∞ is used, because for a wing of infinite span, the induced velocity vanishes and the geometrical angle of attack equals the actual angle of attack.

The secondary flow, however, generates at ξ the induced velocity w perpendicupar to V, so that the wing does not have the geometrical angle of attack γ_∞ but the actual angle of attack (Fig. 2).

$$\gamma = \gamma_\infty - \frac{w}{V}\,.$$

If $c_{a\,\infty\,0}$ represents the lift coefficient in the middle of the

wing, when there is no induced velocity there, then, for ξ,

$$c_a = c_{a\infty o} + k\left(\delta - \frac{w}{V}\right) \qquad (9)$$

Taking account of equation (9), equation (8) becomes

$$\Gamma_o\sqrt{1-\xi^2}\,(1+\alpha\,\xi^2+\beta\,\xi^4) = \left(\frac{c_{a\infty o}}{2}+\frac{k}{2}\,\delta\right)Vt - \frac{k}{2}\,w\,t \qquad (8a)$$

This shows that the wing form $t\,(\xi)$ is not fixed, but depends on the wing warping $\delta\,(\xi)$ for a given circulation distribution.

a) The flat wing.- We will confine ourselves to the flat unwarped wing, which has the same geometrical angle of attack $\gamma_{\infty o} = \gamma_{\infty \xi} = \gamma_\infty$. On taking equation (3) into consideration, equation (8a) reads

$$\Gamma_o\sqrt{1-\xi^2}\,(1+\alpha\,\xi^2+\beta\,\xi^4) = \frac{c_\infty}{2}\,V\,t -$$

$$\Gamma_o\,\frac{kt}{4b}\left[1+\alpha\left(3\,\xi^2-\frac{1}{2}\right)+\beta\left(5\,\xi^4-\frac{3}{2}\,\xi^2-\frac{1}{16}\right)\right] \qquad (8b)$$

and, solved according to t,

$$t = \frac{\sqrt{1-\xi^2}\,(1+\alpha\,\xi^2+\beta\,\xi^4)}{\frac{c_{a\infty}\,V}{2\,\Gamma_o} - \frac{k}{4b}\left[1+\alpha\left(3\,\xi^2-\frac{1}{2}\right)+\beta\left(5\,\xi^4-\frac{3}{2}\,\xi^2-\frac{1}{16}\right)\right]}$$

Then

$$\Gamma_o = \frac{c_{a\infty o}}{2}\,Vt_o - \frac{k}{2}\,w_o\,t_o = \frac{c_{a\infty o}}{2}\,Vt_o - \Gamma_o\,\frac{kt_o}{4\,b}\left(1-\frac{\alpha}{2}-\frac{\beta}{16}\right) \qquad (8c)$$

from which we obtain

$$\frac{t}{t_o} = \frac{\sqrt{1 - \xi^2}\,(1 + \alpha\,\xi^2 + \beta\,\xi^4)}{1 - \frac{k}{4}\frac{t_o}{b}\left[3\,\alpha\,\xi^2 + \beta\left(5\,\xi^4 - \frac{3}{2}\,\xi^2\right)\right]} \qquad (9)$$

For the flat wing the circulation distribution is therefore independent of the angle of attack and $t\,(\xi)$ is a function of the ratio of the central chord to the span for a given circulation distribution.

The application is best illustrated by an example. It is desired to construct a flat unwarped wing of 40 m (131 ft.) span and 6.5 m (21.3 ft.) central chord, so that, with a thick profile (No. 449 of the Göttingen collection), the thickness is 1.1 m (3.6 ft.).* The circulation distribution is characterized by $\alpha = -0.5$ and $\beta = -0.1$, while the theoretical value 2π is used for k.

In Figure 6a the circulation Γ, the chord t and the induced velocity w are plotted along the half-span, and indeed all as ratios to the values in the center of the wing. Figure 7a represents a practical contour for the calculated wing chords. Figure 7b gives, for comparison, the wing of minimum induced drag with the same area and span, which must have the elliptical form.

The comparison of the induced drag, bending moments and torsional moments of both wings is now of interest. If we mark all the symbols referring to the elliptical wing with an asterisk

*L. Prandtl, "Ergebnisse der Aerodynamischen Versuchsanstalt zu Göttingen," Report I, Oldenbourg, Munich and Berlin, 1921.

and compare the ratios for the same lift, which alone has sense, we obtain, from equation (2)

$$\Gamma_o = \frac{4\ A}{\pi\ \rho\ b\ V\left(1 + \frac{\alpha}{4} + \frac{\beta}{8}\right)}$$

$$\Gamma_o' = \frac{4\ A}{\pi\ \rho\ b\ V}$$

$$\frac{W_i}{W_{i\ min}} = \frac{1 + \frac{\alpha}{2} + \frac{\beta}{4} + \frac{\alpha^2}{4} + \frac{11}{32}\ \alpha\ \beta + \frac{\beta^2}{128}}{\left(1 + \frac{\alpha}{4} + \frac{\beta}{8}\right)^2} \tag{10}$$

$$\frac{M_o}{M_o'} = \frac{1 + \frac{2}{5}\ \alpha + \frac{8}{35}\ \beta}{1 + \frac{1}{4}\ \alpha + \frac{1}{8}\ \beta} \tag{11}$$

According to Figure 8, therefore, the chosen circulation distribution exceeds the minimum drag by 8.2%, but reduces the bending moment by 9.9% and increases the torsional moment in diving flight by 14.1%. In this connection, however, it should be noted that the elliptical wing, likewise with 163 m^2 area in the middle, has a chord of only 5.19 m and a height of only 0.88 m against t_o = 6.5 m and h_o = 1.1 m of the wing used for comparison. Moreover, the induced drag is only a portion of the total drag, 5 to 15% in straightaway flight and 20 to 30% in climbing, so that the drag increment, especially in flight with with small c_a, has a still much smaller percentile value.

Figures 6a and 6b also show the course of the bending and torsional moment along the span. Diving flight, i.e., the angle

of attack with zero lift, was chosen for the comparison of the torsional moments. In this case, the induced velocity for each element $t\,dx$ of the wing is also zero, and each element has the same moment coefficient c_m ($c_a = 0$) and yields a torsional moment of

$$d\,T = c_{m(ca=o)}\,\frac{\rho}{2}\,V^2\,t^2\,d\,x$$

so that this becomes

$$T\,(\xi) = \frac{\rho}{2}\,V^2\,\frac{b}{2}\,c_{m(ca=0)}\int_{\xi}^{1} t^2\,d\,\xi \qquad (12)$$

We now introduce t from equation (9). The resulting integral is not solvable mathematically, however, and is best solved graphically by planimetry for the surface area

$$F = \frac{b}{2}\int_{-1}^{+1} t\,d\,\xi \qquad (13)$$

Figure 9a shows another wing with the same circulation distribution as the wing in Figure 7a, but with a different t_o/b. The corresponding elliptical wing of like area and span (Fig. 9b) stands, as regards drag and bending moment, in the same relation to it as the two other wings, but with a slightly different torsional moment.

Corresponding to the circulation distribution of Figures 4a, 4b, and 4c, Figure 10 shows the drags and bending moments as compared with the wing having an elliptical distribution.

b) The warped wing.- A given circulation distribution can be produced not only by a flat wing whose chord is determined by equation (9), but also by a suitable warping, within certain limits, of a wing of any other form.

Assuming the wing contour $t\ (\xi)$, we now seek the wing warping $\delta\ (\xi)$ required to produce the desired lift distribution. We arrive at the solution indirectly, by first calculating the lift coefficients $c_{a\,\infty}$ corresponding to the geometrical angles of attack $\gamma_\infty = \gamma_{\infty\,0} + \delta\ (\xi)$ and then proceeding, according to the experimentally known relation between c_a and γ, to γ_∞ and then to δ.

If we eliminate Γ_0 from equations (8b) and (8c) and solve them according to $c_{a\,\infty}$, we obtain

$$c_{a\,\infty} = c_{a\,\infty\,o}\,\frac{t_o}{t}\,\times$$

$$\frac{\sqrt{1-\xi^2}\,(1+\alpha\xi^2+\beta\xi^4) + \frac{kt}{4b}\left[1+\alpha\left(3\,\xi^2-\frac{1}{2}\right)+\beta\left(5\,\xi^4-\frac{3}{2}\,\xi^2-\frac{1}{16}\right)\right]}{1+\frac{k\,t_o}{4\,b}\left(1-\frac{\alpha}{2}-\frac{\beta}{16}\right)} \qquad (14)$$

The relation $c_{a\infty}\,(\gamma_\infty)$ is plotted in Figure 11 for the profile No. 449 on which the following examples are based. The measurements of the Göttingen model wing refer to the so-called normal wing with an aspect ratio of $\frac{F}{b^2} = \frac{1}{5}$. For our purposes, therefore, the measured angle of attack must be converted by calculation to the corresponding angle for a wing of infinite span with no induced velocity, whose angle of attack, on the assumption of

elliptical distribution, is smaller than that of the model wing by the amount

$$\left(\frac{w}{v}\right)^{o} = \Delta\gamma^{o} = 57.3\,\frac{c_a}{2\pi}\,\frac{F}{b^2} = 1.823\,c_a$$

the number 57.3^{o} being obtained by the conversion of the circular measure into angular measure, $2\pi = 360^{o}$ and hence

$$1 = \frac{360^{o}}{2\pi} = 57.3^{o}$$

If a fixed $c_{a\,\infty\,o}$ is prescribed in the center of the wing, then the $c_{a\,\infty}$ required for the production of the desired circulation distribution is everywhere known through equation (14) and Figure 11. The geometrical angle of attack corresponding to every value of $c_{a\,\infty}$ can be read from Figure 11, and the angle of decalage δ can be obtained from the formula

$$\gamma_{\infty} = \gamma_{\infty\,o} + \delta$$

The statement of $\gamma_{\infty\,o}$ suffices to characterize the geometric angle of attack of the wing.

Figure 12 shows the relations for a tapered wing (Fig. 13) with a rectangular middle section, which agrees in area and span with Figures 7a and 7b and which, moreover, is supposed to have the same circulation distribution as Figure 7a. The outermost wing section must accordingly be set 9^{o} less steep than the middle section.

For the flat wing, the circulation distribution along the span is the same for all angles of attack, so long as c_a var-

ies proportionally with the angle of attack. This does not hold true for the warped wing. The latter has, along the span, quite different lift coefficients, which, due to their linear dependence on the angle of attack, cannot change to an equal per cent with the changing of the latter. In the case of a nonelliptical flat wing, slight discrepancies occur in the lift coefficients, due to variations in the induced velocities, but, with variations in the angle of attack, the induced velocities always vary by such amounts that the lift distribution remains unchanged. In the case of a warped wing, the more the angle of attack $\gamma_{\infty o}$ recedes from the above-considered "fundamental value," just so much more the circulation distribution will differ from the "fundamental distribution," i.e., the coefficients α and β, which characterize them, will assume other values, which we now have to determine.

Approximation of the Lift Distribution for Given Wings

Only a limited variety of lift distributions can be represented by the two parameters α and β. The distribution for any given wing generally requires other parameters and, if strictly taken, an infinite number of them. In practice, however, two parameters often give a close enough approximation, if so chosen that the distribution characterizing them corresponds as nearly as possible to the actual. This applies especially to distributions which are more difficult to determine than the elliptical ones are, as generated by tapered wings.

By two parameters we obtain complete agreement in four points along the half-span, namely, in the middle of the wing and at the tips, where the circulation must sink to zero and also for any two selected intervening points. For these intermediate values ξ_1 and ξ_2 we are in the position to establish two conditional equations whose solution will give the desired parameters α and β.*

a) The warped wing.- For the development of the conditional equations, we introduce into equation (14) the values of $c_{a\,\infty\,o}$, $c_{a\,\infty}$, t_o and t first for ξ_1 and then for ξ_2 corresponding to a definite $\gamma_{\infty\,o}$, thus obtaining two equations of the form

$$\begin{aligned} A_1 - \alpha B_1 - \beta C_1 &= 0 \\ A_2 - \alpha B_2 - \beta C_2 &= 0 \end{aligned} \qquad (15)$$

with α and β as unknown quantities. In the above equations

$$A_1 = \frac{c_{a\,\infty\,1}\ t_1}{c_{a\,\infty\,o}\ t_o} + \frac{kt_1}{4\ b}\left(\frac{c_{a\,\infty\,1}}{c_{a\,\infty\,o}} - 1\right) - \sqrt{1 - \xi_1^2} \qquad (16)$$

$$B_1 = \frac{kt_1}{8\ b}\left(\frac{c_{a\,\infty\,1}}{c_{a\,\infty\,o}} - 1\right) + \frac{kt_1}{4\ b}\ 3\ \xi_1^2 + \xi_1^2\sqrt{1 - \xi_1^2} \qquad (17)$$

$$C_1 = \frac{kt_1}{64b}\left(\frac{c_{a\,\infty\,1}}{c_{a\,\infty\,o}} - 1\right) + \frac{kt_1}{4\ b}\left(5\ \xi_1^4 - \frac{3}{2}\ \xi_1^2\right) + \xi_1^4\sqrt{1 - \xi_1^2} \qquad (18)$$

and A_2, B_2, and C_2 are formed by exchanging $c_{a\,\infty\,1}$, t_1

*The problem is treated according to the same line of reasoning although in a formally different way, by Glauert in his book "The Elements of Aerofoil and Airscrew Theory," Cambridge, 1926 (recently published also in German by Springer). His theorems are used by Küssner in his dissertation "Das wirtschaftliche Ozeanflugzeug," Zeitschrift fur Flugtechnik und Motorluftschiffahrt, 1928, p. 513.

and ξ_1 for $c_{a\,\infty\,2}$, t_2, and ξ_2. In the example, for $c_{a\,\infty\,o} = 0.4$ according to equation (11), $\gamma_{\infty\,o} = -4.2^\circ$. In $\xi_1 = 0.5$, according to Figure 12, $\delta_1 = -0.4^\circ$. Hence $\gamma_{\infty\,1} = -4.6^\circ$ and, from Figure 11, $c_{a\,\infty\,1} = 0.365$. It is preferable to choose 0.5 to 0.6 for ξ_1 and 0.85 to 0.95 for ξ_2.

The true lift coefficient of the whole wing is obtained by combining equations (2) and (8c) to

$$c_a = c_{a\,\infty\,o}\,\frac{\pi}{4}\,\frac{b\,t_o}{F}\,\frac{1+\frac{\alpha}{4}+\frac{\beta}{8}}{\left[1+\frac{k\,t_o}{4\,b}\left(1-\frac{\alpha}{2}-\frac{\beta}{16}\right)\right]} \qquad (19)$$

while the coefficient of the induced drag is obtained from equations (4) and (8c).

$$c_{wi} = c_{a\,\infty\,o}^2\,\frac{\pi}{16}\,\frac{t_o^2}{F}\,\frac{\left(1+\frac{\alpha}{2}+\frac{\beta}{4}+\frac{\alpha^2}{4}+\frac{11}{32}\,\alpha\,\beta+\frac{\beta^2}{128}\right)}{\left[1+\frac{k\,t_o}{4\,b}\left(1-\frac{\alpha}{2}-\frac{\beta}{16}\right)\right]^2} \qquad (20)$$

In Figure 14 there are plotted the results of the calculation for $\xi_1 = 0.5$ and $\xi_2 = 0.9$ for the wing shown in Figure 13. It is obvious from Figure 15, which shows the lift distribution for several angles of attack that, for lift coefficients greater than the "fundamental value," the lift distribution is fuller and approaches the most favorable form but, for smaller lift coefficients, continually recedes from the elliptical form. In particular, the induced drag no longer vanishes for zero lift. This is also to be expected, since, in the case of a warped wing, zero lift is not due to the fact, as in the case of a flat wing,

that all the elements of the wing produce no lift and hence no secondary currents, but that a portion of the wing (for the present example, the inner portion) produces some lift, which is offset, however, by the negative lift of the outer portion of the wing. This lift distribution, which differs considerably from the elliptical, produces secondary flows and, consequently, induced drag. Figure 16 represents the induced drags of the three wings shown in Figures 7a, 7b, and 13 in the form of polars. In order to render the differences more obvious, a larger scale than usual was taken for c_{wi}.

b) The flat wing.- The lift distribution of a given flat wing is determined approximately by the solution of two linear equations (15), as represented above for the warped wing. Since $c_{a\,\infty\,o} = c_{a\,\infty\,1} = c_{a\,\infty\,2}$, the expressions for A, B and C are simplified to/

$$A_1 = \frac{t_1}{t_o} - \sqrt{1 - \xi_1^2} \qquad (16a)$$

$$B_1 = \xi_1^2 \left(\frac{3k}{4} \frac{t_1}{b} + \sqrt{1 - \xi_1^2} \right) \qquad (17a)$$

$$C_1 = \frac{k\,t_1}{4\,b} \left(5\,\xi_1^4 - \frac{3}{2}\,\xi_1^2 \right) + \xi_1^4 \sqrt{1 - \xi_1^2} \qquad (18a)$$

and similar values for A_2, B_2, and C_2.

General Remarks

The derived formulas are based on the linear dependence of the lift on the angle of attack and on the assumption that the

induced velocities w must be small in comparison with the flight speed V. In general, both conditions are sufficiently fulfilled, i.e., so long as no separation of the flow takes place on the suction (upper) side of the wing. This separation of the flow, like the second part of the wing drag (the profile drag) is due to viscosity effects and is not yet satisfactorily calculable. We must content ourselves, therefore, with a few qualitative statements. The profile drag depends chiefly on the character of the wing surface, the ratio of the thickness to the chord and, other conditions remaining the same, on the Reynolds Number $R = Vt : \nu$ (ν being the kinetic viscosity in m^2/s). In general, the greater R is, the smaller c_{wp}, and even the separation of the flow is postponed to greater angles of attack. In this respect, a rectangular wing with constant R should give the best results. Tapered wings, on the contrary, have a much smaller R toward their tips than in the middle, and the separation begins at their outer ends. This tendency is considerably increased by the distribution of the induced velocity w. The distribution of the downwash is always such that the lift distribution is approximately elliptical. The tips of a tapered wing are thus more heavily loaded than the middle portion. Due to small or even negative downward velocities at the wing tips, the effective angles of attack are greater there than in the middle, where they are reduced by great downward velocities. As regards the maximum attainable lift, tapered wings may be excelled by

elliptical wings. This surmise is confirmed by a Göttingen wind-tunnel test. Possibly the maximum lift is less affected by the fuselage than in the case of elliptical wings. Reliable information on this point can be obtained only by wind-tunnel tests. Moreover, it is ascribable to this equalizing effect of the downward velocity, that the bending moment of tapered wings is not so small as the plan form alone might lead one to expect.

The downward velocity at the stabilizer is important for the constructor, because it affects the stability. An estimate of its magnitude for a tapered wing can be made by increasing the known downwash correction factor for an elliptical wing by the ratio of the downwash velocities for the tapered and elliptical wings on the wings themselves and based on equal lift, hence, according to equations (2) and (3), by the amount

$$\frac{w}{w'} = \frac{1 + \alpha\left(3\,\xi^2 - \frac{1}{2}\right) + \beta\left(5\,\xi^4 - \frac{3}{2}\,\xi^2 - \frac{1}{16}\right)}{1 + \frac{\alpha}{4} + \frac{\beta}{8}}$$

For ξ we must thereby adopt the value corresponding to 1/3 to 1/2 the half-span of the stabilizer. For stabilizers which are small in comparison with the wing span, ξ may unhesitatingly be put down as zero.

*Helmbold, "Ueber die Berechnung des Abwindes hinter einem rechteckigen Tragflügel," Zeitschrift für Flugtechnik und Motorluftschiffahrt 1925, No. 15, pp. 291-294.

Translation by Dwight M. Miner,
National Advisory Committee
for Aeronautics.

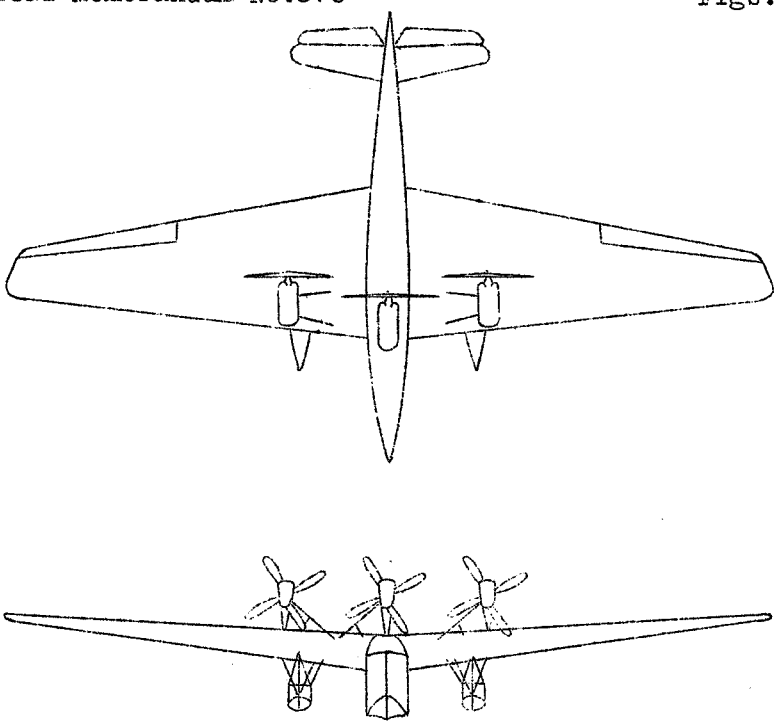

Fig.1 The Rohrbach "Romar" flying boat.

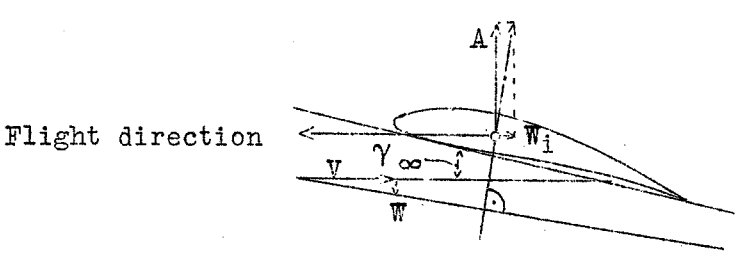

Fig.2 Production of induced drag W_i by changing the angle of attack.

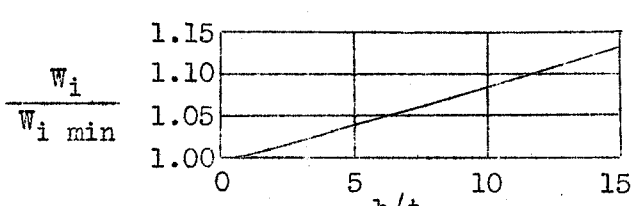

Fig.3 Ratio of induced to minimum drag of rectangular wing plotted against aspect ratio (Betz).

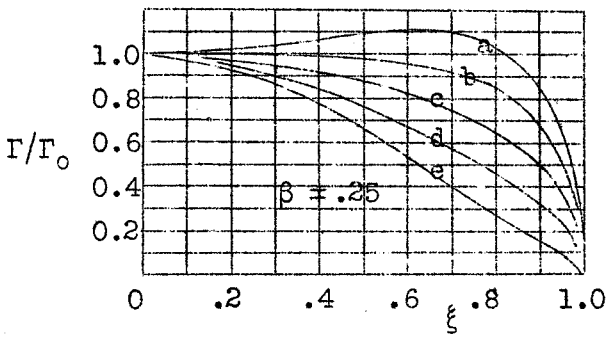

Fig.4a

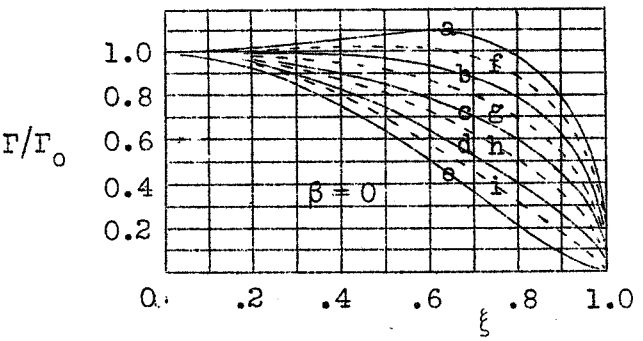

Fig.4b

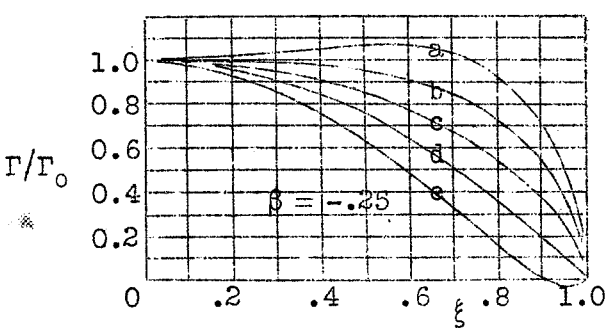

Fig.4c

a, α = 1.0 d, α = -0.5 g, α = 0.25
b, " = 0.5 e, " = -1.0 h, " = -0.25
c, " = 0 f, " = 0.75 i, " = -0.75

Fig.4a,b,c Circulation distributions Γ according to eq.1 along the half-span for different coefficients α and β.

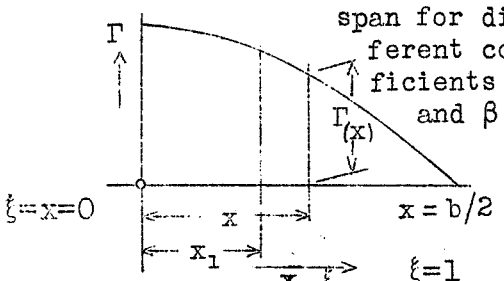

Fig.5 Deduction of bending moment.

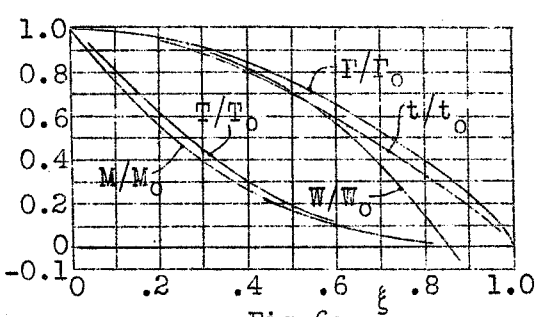

Fig.6a

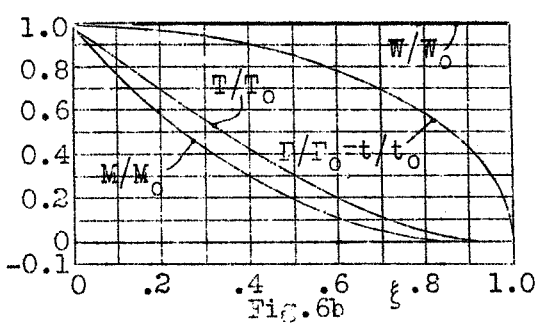

Fig.6b

Fig.6a,b Distribution of circulation, chord, induced velocity, bending and torsional moment along the half-span for a flat wing with:
a, Circulation distribution according to eq.1 for α = 0.5 and β = 0.1;
b, With elliptical circulation distribution.

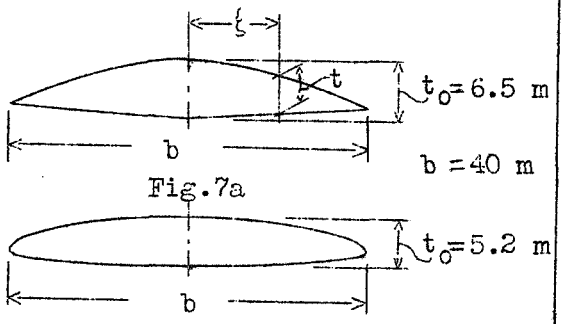

Fig.7a

Fig.7b

Fig.7a,b Wing contours: a,With circulation distribution according to Fig.6a,span 40 m (131 ft.),area 163 m^2(1754.5 sq.ft.) b,Wing of mimimum induced drag, of like span and area.

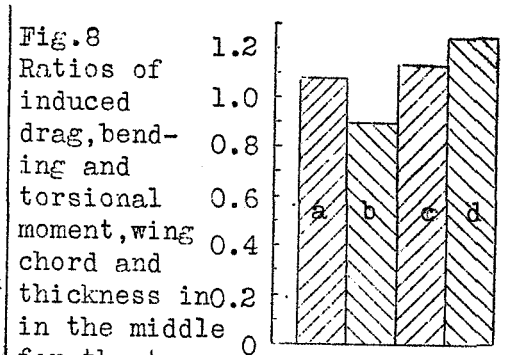

Fig.8 Ratios of induced drag,bending and torsional moment,wing chord and thickness in the middle for the two wings Figs.7a and 7b.
a, $W_i/W_{i\ min}$=1.081 c, T_o/T_o'=1.141
b, M_o/M_o'= 0.901 d, t_o/t_o' = $= h/h_o' = 1.252$

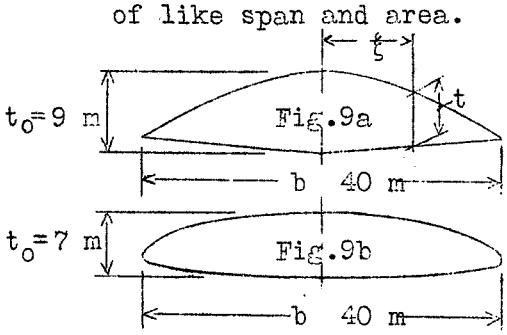

Fig.9a,b Wing contours: a,Wing with same circulation distribution as Fig.6a,but with greater t_o/b;b,Wing of minimum induced drag,with b = 40 m(131 ft.) and F = 220 m^2 (2368 sq.ft.)

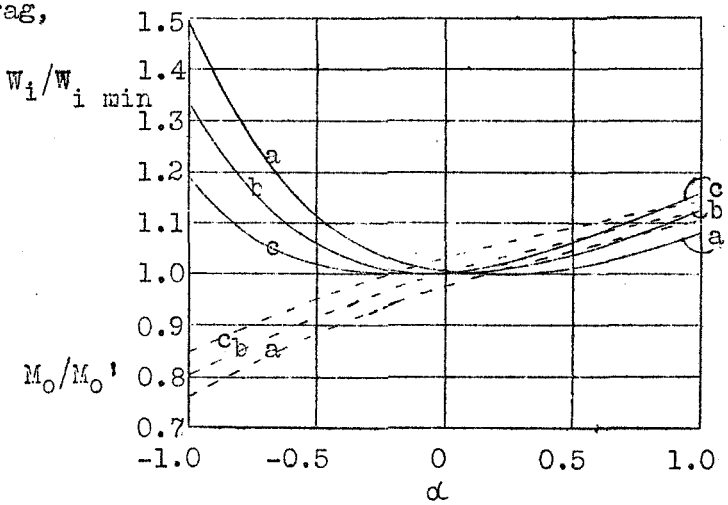

a, β = -0.25
b, β = 0
c, β = +0.25

Fig.10 Drags and bending moments of circulation distributions in Fig.4 in comparison with the drags and bending moments of elliptical distribution.

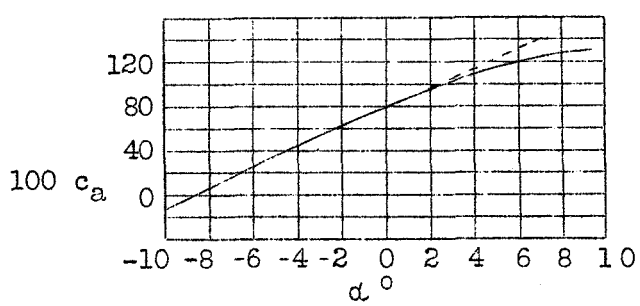

Fig.11 c_a as a function of the angle of attack for Göttingen profile 449 converted to a wing of infinite span.

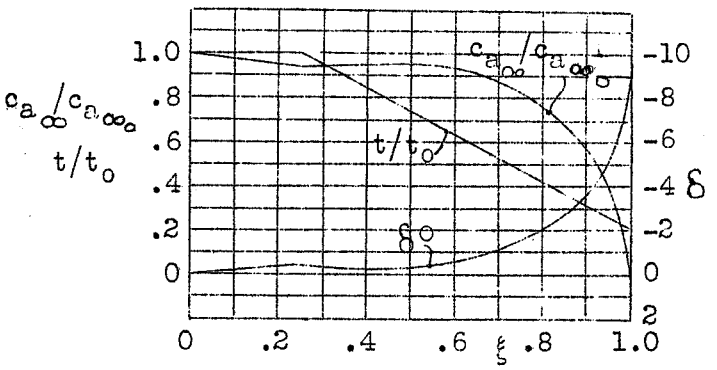

Fig.12 c_{a_∞} and decalage δ along the half-span for the warped tapered wing in Fig.13.

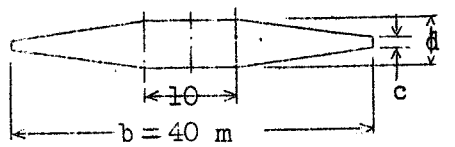

c, 1.2 m d, t_o = 5.4 m

Fig.13 Warped tapered wing with rectangular middle portion. F = 163 m^2 (1754.5 sq.ft.)

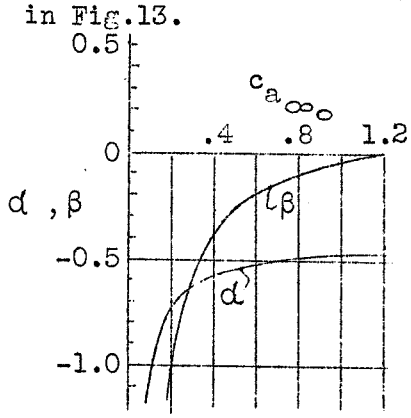

Fig.14 Coefficients α and β in changing the angle of attack for the tapered wing in Fig.13

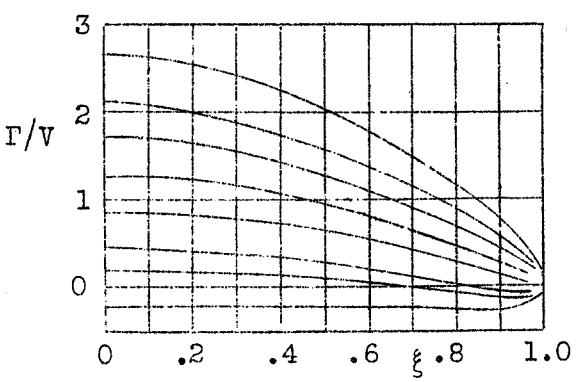

Fig.15 Lift distributions of tapered wing of Fig.13 at different angles of attack.

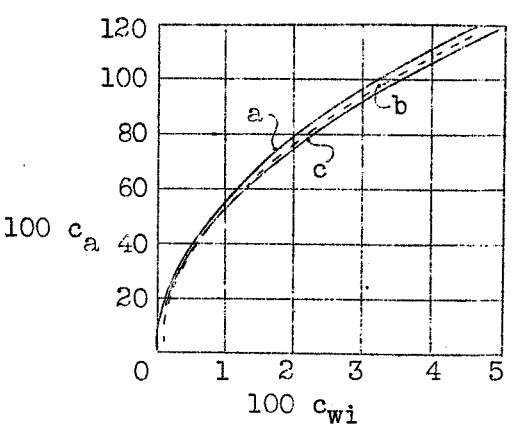

a, Fig.7b
b, Fig.13
c, Fig.7a

Fig.16 Induced drag of wings shown in Figs.7a, 7b, and 13 in the form of polars.